Greenland ice sheet vulnerability under diverse climatic warming scenarios

Benjamin A. Keisling[1,2], Joerg M. Schaefer[2,3], Robert M. DeConto[4], Jason P. Briner[5], Nicolás E. Young[2], Caleb Walcott[5], Gisela Winckler[2,3], Allie Balter-Kennedy[2,3], Sridhar Anandakrishnan[6]

[1]University of Texas Institute for Geophysics, Austin, TX
[2]Lamont-Doherty Earth Observatory, Palisades, NY
[3]Department of Earth and Environmental Sciences, Columbia University, New York, NY
[4]Department of Geosciences, University of Massachusetts Amherst, Amherst, MA
[5]Department of Geology, University at Buffalo, Buffalo, NY
[6]Department of Geosciences, Pennsylvania State University, University Park, PA

ABSTRACT (200 words)

Sea-level rise of even one meter will have drastic global impacts. Melting the Greenland Ice Sheet (GIS) would raise sea level by 7.4 meters. There is an urgent need to improve predictions of how quickly the GIS will contribute its first meter of sea-level rise, and from where on the ice sheet that water will come. Estimating the volume of Greenland ice that was lost during past warm periods offers a way to constrain the ice sheet's likely response to future warming. Here, we assess the sea-level potential across Greenland, based on an ensemble of ice-sheet model simulations that represent a wide range of plausible deglaciation styles. The most vulnerable region of the ice sheet is in West Greenland between approximately 64ºN and 76ºN, ranging from ~10 to ~150 km behind the present-day ice margin. The ensemble spread for the most stable regions of the GIS is sensitive to lithospheric feedbacks, while the most vulnerable GIS region is predominantly sensitive to spatial climatology and precipitation lapse rate. These results can guide future subglacial sampling by identifying regions and locations where such data will have the greatest impact on our understanding of ice-sheet vulnerability/contribution to sea-level rise in a warming world.

Sea-level rise (SLR) is one of the most profound economic, social and environmental issues facing humanity today. The flooding alone associated with ongoing sea-level rise is projected to cost up to 3% of global GDP annually (27 trillion US dollars) by the end of this century if emissions continue unabated (Jevrejeva et al. 2018). In the United States, sea-level rise will disproportionately impact communities of color and those in low-income areas, exacerbating issues of environmental justice (Hardy et al. 2017). Globally, the displacement of hundreds of millions of people will have cascading social, political, and environmental impacts as populations in low-lying areas, especially in the global south, are forced inland by rising seas (Geisler & Currens 2017). Where future sea-level rise will originate is critical to adaptation, because the spatial pattern of ice loss impacts that of sea-level rise (Larour et al. 2017).

The rate of global SLR has nearly tripled since 1890 and has continued to accelerate over the satellite era (Hay et al. 2015, Nerem et al. 2018). The relatively modest rates of SLR in the 19th and most of the 20th centuries were driven primarily by increased oceanic heat uptake of the anthropogenic warming (Hay et al. 2015) and retreating mountain glaciers (Oerlemans 1994). In the late 20th century, SLR accelerated as glacier retreat increased globally (Hugonnett et al. 2021). In the last two decades, the melting of the Greenland ice sheet (GIS) emerged as a key driver of SLR (Mouginot et al. 2019).

The acceleration of the GIS contribution to SLR is very likely caused by human perturbations to the global climate system (IPCC, 2019). We can look to past responses of the GIS to naturally forced periods of global warmth to understand what might be in store for future decades and centuries (Briner et al. 2020). Under natural occurring conditions in the recent geologic past, the ice-sheet vanished at least once (Schaefer et al., 2016). The complexity of evidence has historically lead to controversial evaluations of Pleistocene GIS stability (Funder et al. 2001, Jansen & Sjøholm 1991, Bierman et al. 2014, NEEM Community 2013). However, there is a new line of direct observations that points to a significantly less stable ice sheet and documents the absence of the entire ice sheet at least once in the geological past (Schaefer et al. 2016, Christ et al. 2021). Terrestrial sea-level reconstructions have attempted to place constraints on past Pleistocene sea-level highstands (e.g. Dutton et al. 2021), although disentangling the relative contributions of specific ice sheets is difficult when relying on sea-level highstand indicators (Hay et al. 2014), particularly for magnitudes of sea level rise on the order of a few meters (Dyer et al. 2021). Ice-sheet models provide a complementary method for predicting where the first meter of sea level will originate, but differences between ice-sheet models makes it difficult to assess with high confidence which parts of the GIS margin are the most responsive (Plach et al. 2018). Previous studies have used ice-sheet models to quantify the response of the GIS to specific periods of past warmth, and come to different conclusions about the resilience (Helsen et al. 2013) and geometry (e.g. Helsen et al. 2013, Stone et al. 2013, Robinson et al. 2011) of the ice sheet, even for the same Pleistocene interglacial (e.g. Plach et al. 2018). To resolve these problems, we here chose a complementary approach using an ensemble of ice-sheet model simulations.

Here we assess which sectors of the GIS are most vulnerable to warming climate, and thus the most likely source area for the first meter of sea level contribution from the GIS. We use two different starting climatologies representative of warmth driven by greenhouse gasses (modern) versus high boreal summer insolation (Holocene Thermal Maximum; HTM) (Supplemental Figure 1). In addition, by including simulations in our ensemble that start with both modern and LGM configurations, and which experience warming across a range of rates, we can effectively examine the response of the ice sheet to many different deglaciation scenarios, and combine all of the responses to constrain the “sea-level potential” (SLP) of any particular site, which we define as the amount the GIS has contributed to sea level when a particular location on Greenland is ice-free. Our ensemble approach specifically encapsulates multiple sources of uncertainty by capturing different end-members in the climate forcing, initialization, and solid-Earth model, thereby allowing us to place uncertainties on estimates of sea-level potential that stem from these unknowns. Each unique set of parameters is subject to four different rates of atmospheric warming, allowing us to capture how uncertainty in these parameters affects the way the ice sheet retreats under diverse warming scenarios. We map the GIS response to warming, in order to (1) provide a robust estimate of the region(s) of GIS that are most likely to contribute to the first few meters of global sea-level change, (2) guide future sub-glacial access efforts that can provide targeted information about the response of the ice sheet to past warming, and (3) contextualize existing datasets within a glaciologically coherent framework. From our resulting map, we can infer the sea-level potential of any part of the GIS, regardless of when the deglaciation occurred. Stated differently, the map illustrates which segments of the GIS are most vulnerable under diverse climatic warming scenarios.

Figure 1 shows the method that we apply to calculate sea-level potential, and the sensitivity of the sea-level potential to each of our ensemble parameters. For each 10km model grid cell on Greenland, we analyzed the ensemble to find the first time the site became ice-free in each simulation (Figure 1a). For the first ice-free timestep in each simulation, we gather the ice-sheet volume (Figure 1b) and extent (Figure 1c). By doing this for every grid cell, we generate the median contribution to sea-level in our ensemble as well as the spread across all ensemble members (Figure 1b). For each site, we also look at our results along every dimension of our ensemble, enabling us to calculate the importance of each parameter for each site and rank which of the considered parameters are dominant for each site. The sensitivity is defined as the width of the ensemble spread for each parameter separately divided by the width of the full ensemble. The smaller this number, the more that knowledge about that parameter would reduce uncertainty in sea-level potential for that site (Figure 1b). Secondary and tertiary parameter ranks are shown in Supplemental Figure 2.

RESULTS

We find that each of the four parameters we considered (starting geometry, aesthenosphere relaxation time, lapse rate for precipitation, and starting climatology) play a dominant role for specific parts of the ice sheet. The starting climatology and precipitation-lapse rate generally playing a greater role near the ice-sheet margin, and lithospheric response time and initialization playing the dominant role in inland regions (Figure 2a). During initial retreat, some sectors of the ice sheet gain mass in simulations where we apply a lapse rate to precipitation. Towards the end of deglaciation, independent ice caps remain along the southeast coast of Greenland in all simulations. To identify the most important drivers for each region, we generated an estimate of the parameter sensitivity for each of our four ensemble parameters (Figure 2b-e). We find that North and West Greenland are most sensitive to the use of a Holocene Thermal Maximum (HTM) climatology, driven the higher temperatures reconstructed in those sectors (Figure 2a). However, a broad region of Northwest Greenland is most sensitive to the inclusion of a precipitation-lapse rate correction, which is also true of South Greenland. In Central and East Greenland, both the initial state (LGM versus modern) and a more responsive solid-Earth are the main factors that drive variance in the ensemble.

Our results provide insight into the source regions for the first few meters of sea-level rise. We find that for both North and West Greenland, there are broad regions where deglaciation occurs when the ice sheet has contributed 0 to 2 meters to sea level (Figure 3b). However, the uncertainty in our sea level source estimates (ensemble spread) is much greater in North Greenland compared to West Greenland (Figure 3c). We combine our estimated sea-level source with ensemble spread to produce a map that highlights areas that (a) deglaciate when the ice sheet has contributed less than 2 meters to SLR and (b) have a histogram width of less than 1.5 meters (Figure 3c).

DISCUSSION

Our GIS sea-level potential map shows a range of confidence levels (Figure 3c). Some areas have high confidence in how much Greenland contributes to sea level once that area has deglaciated. However, some of these (e.g. Central Greenland, Figure 3b) only inform us that the entire ice sheet has melted, information that is not useful for predicting where the first meter of sea level will originate.

Our analysis reveals areas throughout Greenland that reliably predict GIS response for the first few meters of SLR. Here, we discuss the factors that underlie variability in our ensemble, compare our results with other modeling and observational studies, and consider the implications of our results for other sectors of the scientific community.

Identifying the most vulnerable part of the GIS margin

We find that the regions of the GIS that are most likely to contribute to the first meter of SLR are in West and North Greenland (Figure 3b). However, there is greater spread in our ensemble in North Greenland compared to West Greenland (Figure 3c). Without further constraints on key parameters, melt of the West GIS has the highest likelihood to dominate the first meter of SLR. Both of these regions are most sensitive to the spatial climatology pattern (Figure 2a). The inclusion of a precipitation-lapse rate correction and initializing the simulations with a LGM ice-sheet geometry are the dominant parameters in some sub-regions, for instance in Northwest Greenland and Southwest Greenland. Considering the sensitivities of each individual parameter, the spatial climatology, precipitation-lapse rate, and LGM initialization all play some role in controlling the ensemble spread in the regions of Greenland where the first few meters of SLR are likely to be sourced. In contrast, accounting for an enhanced lithospheric response only impacts the ensemble spread around the most resilient portions of the ice sheet; by the time the ice margin has reached these areas, Greenland has most likely contributed >4 meters to SLR (Figure 3b). Thus, while lithospheric response exerts a dominant control on sea-level potential in some regions, this source of uncertainty is not likely to impact the regions where the first meter of SLR will come from. Sea-level fingerprinting indicates that the region we identify as most vulnerable, i.e. West Greenland between approximately 64ºN and 76ºN, ranging from ~10 to ~150km behind the present-day ice margin, will have the greatest impact (relative to ice loss from other parts of Greenland) on cities in Europe, Alaska, and the Southern Hemisphere (Larour et al. 2017).

Parameters underlying variability and confidence in sea-level potential

Initializing the model with a LGM ice-sheet geometry has the greatest impact in Central Greenland, where the LGM ice sheet is thinner than the modern, due to low LGM precipitation rates. However, this parameter is of secondary importance for North and South Greenland, and has the least impact in the central West Greenland ablation zone. In contrast, a reduced lithosphere relaxation time is only dominant in Central Greenland, around the most resilient part of the ice sheet. This parameter is also more likely to play a role once the ice sheet has already experienced a large volume reduction. This may reflect a critical role for solid-Earth processes in dictating the location of the ice-sheet margin in Central Greenland, and also aligns with a region that has previously been argued to have a higher geothermal flux and a more viscous mantle (Fahnestock et al. 2001, Rohogzhina et al. 2014, Stevens et al. 2016). Neglecting a precipitation-lapse rate has the strongest control on the ensemble in Northwest and South Greenland, where separate ice domes exert a strong control on ice dynamics (Figure 2d). The dominance of the precipitation-lapse rate illustrates the importance of accounting for changes in precipitation as temperature changes for maintaining ice-cover over peripheral ice-domes during periods of deglaciation (such as Northwest and South Greenland). Finally, the use of a HTM climatology influences deglaciation in North, West, and South Greenland. In addition to playing an important role in the modern-day ablation zone of West Greenland, central North-West Greenland is particularly sensitive to this parameter. This area corresponds to the lowest-lying part of Greenland's topography, and is on the ice divide between the northwest dome and the central dome of the ice sheet. The dominance of the climatology here reflects the important role of HTM-like conditions (enhanced warming in the North and West) for driving deglaciation further once the northwest dome has disintegrated.

A major control on patterns and rates of deglaciation is the applied surface mass balance (SMB) forcing (e.g. Plach et al. 2018). In our ensemble, the starting SMB fields, and in particular the spatial extent of the ablation zone, play an important role in ice-sheet geometry during deglaciation across all scenarios and play a dominant role in sea-level potential for much of West and North Greenland. Surface mass balance is difficult to accurately reconstruct, particularly for past interglacial periods (e.g. Helsen et al. 2016). Our approach circumvents direct reconstruction of SMB for a particular interglacial by considering a range of forcings and identifying the range of sea-level potential associated with the uncertainty in the climate forcing. By including both a modern-day and HTM climate forcing, we capture two known modes of interglacial climate in Greenland (e.g. Buizert et al. 2018). However, other modes of surface climate are possible, and may become dominant in the future as previously stable boundary conditions change dramatically (e.g. Koenig et al. 2014, Sellevold et al. 2021). Nevertheless, our results confirm the primacy of correctly predicting the spatial patterns of climate over Greenland (Edwards et al. 2014) for projecting the first meters of future sea-level change.

Comparison with other modeling studies

Ice-sheet modeling experiments investigating GIS response to past warmth have resulted in divergent conclusions about ice-sheet stability.

Our results identify areas in West, Northwest and Northeast Greenland as good predictors of GIS sea-level potential across our ensemble. Many previous studies found that West Greenland responded most strongly to past interglacial warm periods (e.g. Greve 2005, Robinson et al. 2011, Born and Nisancioglu 2012, Helsen et al. 2015, Sommers et al. 2021). At the same time, other studies have found that North Greenland is also highly sensitive to past interglacial warmth (e.g. Stone et al. 2013). Some of these studies show both West and North Greenland responding to past warmth simultaneously (Robinson et al. 2011, Born and Nisancioglu 2012). Our sensitivity-mapping approach allows us to consider how and why these results may differ from other studies that modeled Greenland deglaciation patterns. For example, we find that whether Northern Greenland is an early contributor to SLR is dependent on the choice of a HTM-like climate forcing (Figure 2a). Our approach is distinct because rather than consider one particular warm period, our ensemble encapsulates a range of deglaciation scenarios and treats them all equally likely. This allows us to overcome the challenges associated with perfectly simulating a particular time period in favor of identifying the patterns that hold true regardless of the style of deglaciation, and therefore provide useful insight to the uncertain future of the GIS.

Comparison with other records

Holocene melt records are available in North Greenland, including at NEEM (NEEM Community Members 2013) and Agassiz ice cap (Koerner et al. 1990). The climate record from NEEM also indicates a greater sensitivity to HTM conditions, showing an early Holocene warming of 6ºC, relative to 2º degrees at Summit (Lecavalier 2017, Dahl-Jensen et al. 1998). Our ensemble does not include variations in ocean or indirect sea ice forcing, which likely played a role in past deglaciation scenarios (Koenig et al. 2014, Irvali et al. 2019). At the fjord scale, ocean warming can have a distinctive impact on ice-sheet dynamics and thus should be considered in future work (e.g. Straneo et al. 2009, Wood et al. 2021). However, because the modern GIS is mostly terrestrial, ocean forcing is not expected to have a major impact on deglaciation in the future.

The terrestrial sea-level record provides an alternative way to infer GIS stability (e.g. Dyer et al. 2021). However, far-field records are more likely to record extreme sea-level highstands, because modest or transient changes in sea-level tend to be overprinted by transgressions; in contrast, regressive sequences are more likely to remain visible in the stratigraphic record, and far-field reconstructions have yet to yield sea-level fingerprints that differentiate between different sectors of the GIS. Our approach complements far-field sea-level records by providing a method to assess where the first few meters of sea-level rise from Greenland are likely to originate, regardless of the final geometry of the ice sheet at the time of maximum retreat during an interglacial. Terrestrial records from West Greenland have revealed this area was particularly sensitive to warming during the HTM (e.g. Larsen et al. 2016, Young et al., 2021) and our results confirm this as a persistent feature of GIS response to warming.

Our results reveal regions of the GIS which, when ice-free, are associated with a wide range of ice-sheet geometries, and regions where ice-free conditions are associated with a tightly constrained window of sea-level change. Future efforts, including a recently funded program to collect samples from beneath the ice-sheet margin to characterize when different sectors of Greenland were ice-free, in combination with our results, may provide more robust constraints on paleo sea level than have been possible with other methods. Our results reveal distinct spatial patterns of ice-sheet sensitivity to different physical processes, which can provide input to scientific communities working on understanding these processes in space and time; for highly vulnerable regions of GIS, the spatial climatology pattern, treatment of precipitation-lapse rate, and ice-sheet initialization are all important for determining the style of deglaciation. Thus, efforts to more tightly constrain these parameters will reduce uncertainty in sea-level projections for both paleo and future scenarios. Our results provide a foundation for sea-level fingerprinting and local sea-level impact predictions, which can inform vital efforts to enhance coastal community resilience as Earth's climate continues to warm.

ONLINE METHODS

Previous studies have used ice-sheet models to quantify the response of the GIS to specific periods of past warmth, and come to different conclusions about the resilience (Helsen et al. 2013) and geometry (e.g. Helsen et al. 2013, Stone et al. 2013, Robinson et al. 2011) of the ice sheet. Differences in the modeled footprint of the ice sheet are mostly caused by differences in the experimental design, and the approach taken to climate forcing (Plach et al. 2018). However, the relative role of different processes and forcings, including uncertainty in surface mass balance, solid-Earth feedbacks, and ice-sheet initialization has not been fully assessed (Edwards et al. 2014).

Our ensemble approach specifically encapsulates multiple sources of uncertainty in the climate forcing, initialization, and solid-Earth model, thereby allowing us to place uncertainties on estimates of sea-level potential that stem from these unknowns. We use two different starting climatologies representative of warmth driven by greenhouse gasses (modern) versus high boreal summer insolation (Holocene Thermal Maximum; HTM). These climates show different distributions of surface melting and precipitation, allowing us to account for some of the uncertainty in the spatial distribution of these parameters during past deglaciation scenarios and serve as end-members for known warm climate states upon which we prescribe a linear warming ramp. In addition, by including simulations in our ensemble that start with both modern and LGM configurations, and which experience warming across a range of rates, we can effectively examine the response of the ice sheet to many different deglaciation scenarios, and combine all of the responses to constrain the sea-level potential of any particular site. Furthermore, the inclusion of different response rates for the elastic lithosphere, relaxing asthenosphere solid-Earth model allows us to examine the role that the lithosphere might play in modulating the ice-sheet response to deglaciation.

A. Ice-sheet model

We used a three-dimensional thermomechanical ice sheet model that uses a hybrid ice-flow law that efficiently bridges between fast-flowing areas of streaming ice (Shallow Shelf Approximation) and inland areas of low velocity and high driving stress (Shallow Ice Approximation) (Pollard & DeConto 2012a). The model has been validated against other ice-sheet models under a range of conditions (e.g. Cornford et al. 2020, Pollard & DeConto 2020) and has been used extensively for paleo and future ice-sheet simulations in Antarctica

(DeConto et al. 2021). The model uses a Weertman-type sliding law for basal ice motion and a calving scheme based on the divergence of the ice-flow field. All simulations are run at 10km fixed resolution. Basal sliding coefficients are calculated through an inverse scheme that iteratively adjusts sliding to reduce the mismatch between the modeled and observed ice-sheet geometry (Pollard & DeConto 2012b). This model has been extensively applied to understand paleoclimate scenarios where both the boundary conditions and model forcing differ substantially from modern-day, which is a limitation for many ice sheet models.

Ensemble Design

We ran ninety-six simulations varying four key parameters: starting climatology, lapse rate for precipitation, aesthenosphere relaxation time, and starting geometry. Each combination of parameters was subject to four different rates of interglacial warming. We find that both modern geometries (cold-start and transient spin-up) produce similar results for sea-level potential so we focus our analysis on the cold-start simulations, which match modern day ice extent and thickness more faithfully, resulting in 64 total simulations and allowing us to equally weight starting from a modern or LGM configuration.

Initial climate forcing

A primary control on the spatial pattern of GIS deglaciation is the chosen pattern of surface mass balance (SMB). SMB is reasonably well-known for the last 21 kyr, because during this period ice cores, climate models and modern data overlap (Buizert et al. 2018). Conversely, for most past warm periods before 21 ka there is little known about the precise patterns of SMB. Thus, we select two representative time periods from the Holocene to represent end-members in the SMB forcing (Supplemental Figure 1). First, we select a time slice in the early Holocene at 8.5 ka when summer temperatures were the warmest in Greenland. Due to the orbital configuration driving warmth, northern Greenland had a more developed ablation zone and western Greenland had a reduced ablation zone relative to today. The second time-slice chosen is pre-industrial, with minimal melting in northern Greenland and a well-developed ablation zone in western Greenland. Both forcings come from a hybrid model-data reconstruction that includes seasonally resolved spatial and temporal variability (Buizert et al. 2018).

Lapse rate applied to precipitation

Although the ice-sheet margin may have retreated inland of its present-day position during past warm periods, this does not necessarily mean that the ice sheet had lower volume than today. As climate warms, the atmosphere’s capacity to hold water is enhanced, which can lead to increasing precipitation rates for inland ice-sheet regions (Payne et al. 2021). We account for this by considering a precipitation correction that increases precipitation by 2% per degree of temperature increase in each grid cell. This “precipitation-lapse rate correction" enables us to consider the impact of the feedback between a warming atmosphere and its moisture content/capacity in calculating ice-volume changes. We consider this value to be a plausible upper-bound, as it has been found to accurately reproduce glacial-interglacial changes in precipitation rate (Ritz et al. 2001, Abe-Ouchi et al. 2007). The lower-bound on SMB is determined by not applying the precipitation lapse-rate correction, because there is no compensation for increasing melt.

Rate of interglacial warming

The GIS volume decreased in response to past variations in natural forcing, including orbital changes, changes in ocean circulation, and atmospheric greenhouse gasses. Because the precise mechanisms that drove past climate warming vary among interglacial periods (PAGES 2016) and the precise timing of ice-sheet retreat (prior to the LGM) is largely unconstrained (Schaefer et al. 2016), we leverage the best-studied periods of past ice-sheet retreat to understand possible rates of interglacial climate warming. In particular, during the last deglaciation, Greenland's mean annual temperature increased by ~18 ºC between 18ka and 12ka, an average rate of 3 ºC per millennium (Buizert et al. 2014). However, the total temperature change during the summer season, which is largely responsible for controlling ice-sheet melt, was closer to 12 ºC (Buizert et al. 2018). During the early Holocene, more muted warming (~3 ºC over 3 kyr) drove the GIS to eventually retreat behind its present-day margin in many sectors (e.g. Bennike & Weidick, 2001, Larsen et al. 2016, Young et al., 2021). Thus, to capture a reasonable range of warming rates based on paleoclimate evidence in our ensemble, we subject the ice sheet to an interglacial warming ramp ranging from 0.5 ºC kyr^{-1} to 2.0 ºC kyr^{-1} in increments of 0.5 ºC.

Solid-Earth relaxation time

Solid-Earth dynamics influence ice-sheet stability (Austermann et al. 2015) and have changed beneath Greenland as a function of time (Rogozhina et al. 2016) and potentially in response to fluctuations of the GIS itself (Stevens et al. 2016). We included in our ensemble parametric uncertainty in the treatment of solid-Earth dynamics by simply using end-member? mantle relaxation times of 500 and 3,000 years. The former represents hot, low-viscosity (fast-responding) mantle like that underlying northeast Greenland today (Fahnestock et al. 2001), while the latter is a standard value for relaxation time that has been calibrated against measurements of glacial-isostatic adjustment (Le Meur & Huybrechts 1996, Coulon et al. 2021).

Ice-sheet initialization

Following its expansion to the continental shelf edge at the end of the Last Glacial Maximum (21 ka), the GIS retreated first across the continental shelf and then across land. Rising global CO_2 drove the ice sheet to recede following the LGM and approach its present-day margin (Cuzzone et al. 2019). A warm summer orbit led to continued ice-sheet margin retreat inland from its current position during the HTM (e.g. Young et al. 2021). These two phases of retreat illuminate two distinct ways that Greenland may have deglaciated more fully in the past: either quickly following a glacial period, or after reaching a modern-like "interglacial" state and then continuing to retreat. To capture both these possibilities, we start our simulations from either an ice sheet that has been run to equilibrium with LGM climate conditions, or a modern ice-sheet. For the latter, we ran a set of simulations with a cold-start and a set of simulations that has been spun-up to modern through a glacial cycle (Buizert et al. 2018). To initialize the modern ice sheet, we used an observational data set of ice extent and thickness (Morlighem et al. 2017). To equilibrate the LGM ice sheet, we used the LGM climate forcing from (Buizert et al. 2018) and reduced ocean temperatures by 6ºC to allow the ice sheet to advance to the continental shelf. The ice sheet came to thermal equilibrium with the climate during an 80-kyr spin-up phase.

Parameter Ranking

REFERENCES

Abe-Ouchi, A., T. Segawa, and F. Saito. 2007. "Climatic Conditions for Modelling the Northern Hemisphere Ice Sheets throughout the Ice Age Cycle." *Climate of the Past* 3 (3): 423–38.

Austermann, Jacqueline, David Pollard, Jerry X. Mitrovica, Robert Moucha, Alessandro M. Forte, Robert M. DeConto, David B. Rowley, and Maureen E. Raymo. 2015. "The Impact of Dynamic Topography Change on Antarctic Ice Sheet Stability during the Mid-Pliocene Warm Period." *Geology* 43 (10): 927–30. https://doi.org/10.1130/G36988.1.

Bennike, O. & Weidick, A. Late quaternary history around Nioghalvfjerdsfjorden and Jokelbugten, North-East Greenland. Boreas 30, 205–227 (2001).

Bierman, Paul R., Lee B. Corbett, Joseph A. Graly, Thomas A. Neumann, Andrea Lini, Benjamin T. Crosby, and Dylan H. Rood. 2014. "Preservation of a Preglacial Landscape under the Center of the Greenland Ice Sheet." *Science* 344 (6182): 402–5.

Born, A., and K. H. Nisancioglu. 2012. "Melting of Northern Greenland during the Last Interglaciation." *The Cryosphere* 6 (6): 1239–50. https://doi.org/10.5194/tc-6-1239-2012.

Buizert, C., B. A. Keisling, J. E. Box, F. He, A. E. Carlson, G. Sinclair, and R. M. DeConto. 2018. "Greenland-Wide Seasonal Temperatures During the Last Deglaciation." *Geophysical Research Letters* 45 (4): 1905–14. https://doi.org/10.1002/2017GL075601.

Buizert, Christo, Vasileios Gkinis, Jeffrey P. Severinghaus, Feng He, Benoit S. Lecavalier, Philippe Kindler, Markus Leuenberger, et al. 2014. "Greenland Temperature Response to Climate Forcing during the Last Deglaciation." *Science* 345 (6201): 1177. https://doi.org/10.1126/science.1254961.

Briner, Jason P., Joshua K. Cuzzone, Jessica A. Badgeley, Nicolás E. Young, Eric J. Steig, Mathieu Morlighem, Nicole-Jeanne Schlegel, et al. 2020. "Rate of Mass Loss from the Greenland Ice Sheet Will Exceed Holocene Values This Century." *Nature* 586 (7827): 70–74. https://doi.org/10.1038/s41586-020-2742-6.

Christ, Andrew J., Paul R. Bierman, Joerg M. Schaefer, Dorthe Dahl-Jensen, Jørgen P. Steffensen, Lee B. Corbett, Dorothy M. Peteet, et al. 2021. "A Multimillion-Year-Old Record of Greenland Vegetation and Glacial History Preserved in Sediment beneath

1.4 Km of Ice at Camp Century." *Proceedings of the National Academy of Sciences* 118 (13): e2021442118. https://doi.org/10.1073/pnas.2021442118.

Cornford, Stephen L., Helene Seroussi, Xylar S. Asay-Davis, G. Hilmar Gudmundsson, Rob Arthern, Chris Borstad, Julia Christmann, et al. 2020. "Results of the Third Marine Ice Sheet Model Intercomparison Project (MISMIP+)." *The Cryosphere* 14 (7): 2283–2301. https://doi.org/10.5194/tc-14-2283-2020.

Coulon, Violaine, Kevin Bulthuis, Pippa L. Whitehouse, Sainan Sun, Konstanze Haubner, Lars Zipf, and Frank Pattyn. 2021. "Contrasting Response of West and East Antarctic Ice Sheets to Glacial Isostatic Adjustment." *Journal of Geophysical Research: Earth Surface* 126 (7). https://doi.org/10.1029/2020JF006003.

Cuzzone, Joshua K., Nicole-Jeanne Schlegel, Mathieu Morlighem, Eric Larour, Jason P. Briner, Helene Seroussi, and Lambert Caron. 2019. "The Impact of Model Resolution on the Simulated Holocene Retreat of the Southwestern Greenland Ice Sheet Using the Ice Sheet System Model (ISSM)." *The Cryosphere* 13 (3): 879–93. https://doi.org/10.5194/tc-13-879-2019.

Dahl-Jensen, D., K. Mosegaard, N. Gundestrup, G. D. Clow, S. J. Johnsen, A. W. Hansen, and N. Balling. 1998. "Past Temperatures Directly from the Greenland Ice Sheet." *Science* 282 (5387): 268–71. https://doi.org/10.1126/science.282.5387.268.

Dutton, Andrea, Alexandra Villa, and Peter M. Chutcharavan. 2021. "Compilation of Last Interglacial (Marine Isotope Stage 5e) Sea Level Indicators in the Bahamas, Turks and Caicos, and the East Coast of Florida, USA." Preprint. Geosciences – Palaeooceanography, Palaeoclimatology. https://doi.org/10.5194/essd-2021-391.

Dyer, Blake, Jacqueline Austermann, William J. D'Andrea, Roger C. Creel, Michael R. Sandstrom, Miranda Cashman, Alessio Rovere, and Maureen E. Raymo. 2021. "Sea-Level Trends across The Bahamas Constrain Peak Last Interglacial Ice Melt." *Proceedings of the National Academy of Sciences* 118 (33): e2026839118. https://doi.org/10.1073/pnas.2026839118.

Fahnestock, M. 2001. "High Geothermal Heat Flow, Basal Melt, and the Origin of Rapid Ice Flow in Central Greenland." *Science* 294 (5550): 2338–42. https://doi.org/10.1126/science.1065370.

Flesche Kleiven, H, Eystein Jansen, T Fronval, and T.M. Smith. 2002. "Intensification of Northern Hemisphere Glaciations in the Circum Atlantic Region (3.5--2.4 Ma) -- Ice-Rafted Detritus Evidence." *Palaeogeography, Palaeoclimatology, Palaeoecology* 184: 213–23. https://doi.org/10.1016/S0031-0182(01)00407-2.

Funder, Svend, Ole Bennike, Jens Böcher, Carsten Israelson, Kaj Strand Petersen, and Leifur Símonarson. 2001. "Late Pliocene Greenland - The Kap København Formation in North Greenland." *Bulletin of the Geological Society of Denmark* 48: 117–34.

Geisler, Charles, and Ben Currens. 2017. “Impediments to Inland Resettlement under Conditions of Accelerated Sea Level Rise.” *Land Use Policy* 66 (July): 322–30. https://doi.org/10.1016/j.landusepol.2017.03.029.

Hardy, R. Dean, Richard A. Milligan, and Nik Heynen. 2017. “Racial Coastal Formation: The Environmental Injustice of Colorblind Adaptation Planning for Sea-Level Rise.” *Geoforum* 87 (December): 62–72. https://doi.org/10.1016/j.geoforum.2017.10.005.

Hay, Carling, Jerry X. Mitrovica, Natalya Gomez, Jessica R. Creveling, Jacqueline Austermann, and Robert E. Kopp. 2014. “The Sea-Level Fingerprints of Ice-Sheet Collapse during Interglacial Periods.” Quaternary Science Reviews 87 (March): 60–69. https://doi.org/10.1016/j.quascirev.2013.12.022.

Hay, Carling C., Eric Morrow, Robert E. Kopp, and Jerry X. Mitrovica. 2015. “Probabilistic Reanalysis of Twentieth-Century Sea-Level Rise.” *Nature* 517 (7535): 481–84. https://doi.org/10.1038/nature14093.

Helsen, M. M., W. J. van de Berg, R. S. W. van de Wal, M. R. van den Broeke, and J. Oerlemans. 2013. “Coupled Regional Climate&Ndash;Ice-Sheet Simulation Shows Limited Greenland Ice Loss during the Eemian.” *Climate of the Past* 9 (4): 1773–88. https://doi.org/10.5194/cp-9-1773-2013.

Irvalı, Nil, Eirik V. Galaasen, Ulysses S. Ninnemann, Yair Rosenthal, Andreas Born, and Helga (Kikki) F. Kleiven. 2020. “A Low Climate Threshold for South Greenland Ice Sheet Demise during the Late Pleistocene.” *Proceedings of the National Academy of Sciences* 117 (1): 190–95. https://doi.org/10.1073/pnas.1911902116.

IPCC, 2019: IPCC Special Report on the Ocean and Cryosphere in a Changing Climate [H.-O. Pörtner, D.C. Roberts, V. Masson-Delmotte, P. Zhai, M. Tignor, E. Poloczanska, K. Mintenbeck, A. Alegría, M. Nicolai, A. Okem, J. Petzold, B. Rama, N.M. Weyer (eds.)]. In press.

Jevrejeva, S, L P Jackson, A Grinsted, D Lincke, and B Marzeion. 2018. “Flood Damage Costs under the Sea Level Rise with Warming of 1.5 °C and 2 °C.” *Environmental Research Letters* 13 (7): 074014. https://doi.org/10.1088/1748-9326/aacc76.

Koenig, S. J., R. M. DeConto, and D. Pollard. 2014. “Impact of Reduced Arctic Sea Ice on Greenland Ice Sheet Variability in a Warmer than Present Climate.” *Geophysical Research Letters* 41 (11): 3933–42. https://doi.org/10.1002/2014GL059770.

Koerner, R. M., and D. A. Fisher. 1990. “A Record of Holocene Summer Climate from a Canadian High-Arctic Ice Core.” *Nature* 343 (6259): 630–31. https://doi.org/10.1038/343630a0.

Larour, Eric, Erik R. Ivins, and Surendra Adhikari. 2017. “Should Coastal Planners Have Concern over Where Land Ice Is Melting?” *Science Advances* 3 (11): e1700537.

Larsen, Nicolaj K., Jesper Find, Anders Kristensen, Anders A. Bjørk, Kristian K. Kjeldsen, Bent V. Odgaard, Jesper Olsen, and Kurt H. Kjær. 2016. “Holocene Ice Marginal

Fluctuations of the Qassimiut Lobe in South Greenland." *Scientific Reports* 6 (March): 22362. https://doi.org/10.1038/srep22362.

Larsen, Nicolaj K., Laura B. Levy, Anders E. Carlson, Christo Buizert, Jesper Olsen, Astrid Strunk, Anders A. Bjørk, and Daniel S. Skov. 2018. "Instability of the Northeast Greenland Ice Stream over the Last 45,000 Years." *Nature Communications* 9 (1). https://doi.org/10.1038/s41467-018-04312-7.

Lecavalier, Benoit S., David A. Fisher, Glenn A. Milne, Bo M. Vinther, Lev Tarasov, Philippe Huybrechts, Denis Lacelle, et al. 2017. "High Arctic Holocene Temperature Record from the Agassiz Ice Cap and Greenland Ice Sheet Evolution." Proceedings of the National Academy of Sciences 114 (23): 5952–57. https://doi.org/10.1073/pnas.1616287114.

Le Meur, Emmanuel, and Philippe Huybrechts. 1996. "A Comparison of Different Ways of Dealing with Isostasy: Examples from Modelling the Antarctic Ice Sheet during the Last Glacial Cycle." *Annals of Glaciology* 23.

Morlighem, M., C. N. Williams, E. Rignot, L. An, J. E. Arndt, J. L. Bamber, G. Catania, et al. 2017. "BedMachine v3: Complete Bed Topography and Ocean Bathymetry Mapping of Greenland From Multibeam Echo Sounding Combined With Mass Conservation: BEDMACHINE GREENLAND V3." *Geophysical Research Letters*, November. https://doi.org/10.1002/2017GL074954.

NEEM community members. 2013. "Eemian Interglacial Reconstructed from a Greenland Folded Ice Core." *Nature* 493 (7433): 489–94. https://doi.org/10.1038/nature11789.

Nerem, R. S., B. D. Beckley, J. T. Fasullo, B. D. Hamlington, D. Masters, and G. T. Mitchum. 2018. "Climate-Change–Driven Accelerated Sea-Level Rise Detected in the Altimeter Era." *Proceedings of the National Academy of Sciences* 115 (9): 2022–25. https://doi.org/10.1073/pnas.1717312115.

Oerlemans, Johannes. 1994. "Quantifying Global Warming from the Retreat of Glaciers." *Science* 264 (5156): 243–45. https://doi.org/10.1126/science.264.5156.243.

Past Interglacials Working Group of PAGES. 2016. "Interglacials of the Last 800,000 Years." *Reviews of Geophysics* 54 (1): 162–219. https://doi.org/10.1002/2015RG000482.

Payne, Antony J., Sophie Nowicki, Ayako Abe-Ouchi, Cécile Agosta, Patrick Alexander, Torsten Albrecht, Xylar Asay-Davis, et al. 2021. "Future Sea Level Change Under Coupled Model Intercomparison Project Phase 5 and Phase 6 Scenarios From the Greenland and Antarctic Ice Sheets." *Geophysical Research Letters* 48 (16). https://doi.org/10.1029/2020GL091741.

Pollard, D., and R. M. DeConto. 2012a. "A Simple Inverse Method for the Distribution of Basal Sliding Coefficients under Ice Sheets, Applied to Antarctica." *The Cryosphere* 6 (5): 953–71. https://doi.org/10.5194/tc-6-953-2012.

Pollard, D., and R. M. DeConto. 2012b. “Description of a Hybrid Ice Sheet-Shelf Model, and Application to Antarctica.” *Geoscientific Model Development* 5 (5): 1273–95. https://doi.org/10.5194/gmd-5-1273-2012.

Pollard, David, and Robert M. DeConto. 2020. “Improvements in One-Dimensional Grounding-Line Parameterizations in an Ice-Sheet Model with Lateral Variations (PSUICE3D v2.1).” *Geoscientific Model Development* 13 (12): 6481–6500. https://doi.org/10.5194/gmd-13-6481-2020.

Ritz, Catherine, Vincent Rommelaere, and Christophe Dumas. 2001. “Modeling the Evolution of Antarctic Ice Sheet over the Last 420,000 Years: Implications for Altitude Changes in the Vostok Region.” *Journal of Geophysical Research: Atmospheres* 106 (D23): 31943–64. https://doi.org/10.1029/2001JD900232.

Robinson, A., R. Calov, and A. Ganopolski. 2011. “Greenland Ice Sheet Model Parameters Constrained Using Simulations of the Eemian Interglacial.” *Climate of the Past* 7 (2): 381–96. https://doi.org/10.5194/cp-7-381-2011.

Rogozhina, Irina, Alexey G. Petrunin, Alan P. M. Vaughan, Bernhard Steinberger, Jesse V. Johnson, Mikhail K. Kaban, Reinhard Calov, Florian Rickers, Maik Thomas, and Ivan Koulakov. 2016. “Melting at the Base of the Greenland Ice Sheet Explained by Iceland Hotspot History.” *Nature Geoscience* 9 (5): 366–69. https://doi.org/10.1038/ngeo2689.

Schaefer, Joerg M., Robert C. Finkel, Greg Balco, Richard B. Alley, Marc W. Caffee, Jason P. Briner, Nicolas E. Young, Anthony J. Gow, and Roseanne Schwartz. 2016. “Greenland Was Nearly Ice-Free for Extended Periods during the Pleistocene.” *Nature* 540 (7632): 252–55. https://doi.org/10.1038/nature20146.

Sellevold, Raymond, Jan T. M. Lenaerts, and Miren Vizcaino. 2021. “Influence of Arctic Sea-Ice Loss on the Greenland Ice Sheet Climate.” *Climate Dynamics*, July. https://doi.org/10.1007/s00382-021-05897-4.

Sommers, Aleah N., Bette L. Otto-Bliesner, William H. Lipscomb, Marcus Lofverstrom, Sarah L. Shafer, Patrick J. Bartlein, Esther C. Brady, et al. 2021. “Retreat and Regrowth of the Greenland Ice Sheet During the Last Interglacial as Simulated by the CESM2-CISM2 Coupled Climate–Ice Sheet Model.” *Paleoceanography and Paleoclimatology* 36 (12). https://doi.org/10.1029/2021PA004272.

Stevens, Nathan T., Byron R. Parizek, and Richard B. Alley. 2016. “Enhancement of Volcanism and Geothermal Heat Flux by Ice-Age Cycling: A Stress Modeling Study of Greenland.” *Journal of Geophysical Research: Earth Surface* 121 (8): 1456–71. https://doi.org/10.1002/2016JF003855.

Straneo, Fiammetta, and Patrick Heimbach. 2013. “North Atlantic Warming and the Retreat of Greenland’s Outlet Glaciers.” *Nature* 504 (7478): 36–43. https://doi.org/10.1038/nature12854.

Wood, Michael, Eric Rignot, Ian Fenty, Lu An, Anders Bjørk, Michiel van den Broeke, Cilan Cai, et al. 2021. "Ocean Forcing Drives Glacier Retreat in Greenland." *Science Advances* 7 (1): eaba7282. https://doi.org/10.1126/sciadv.aba7282.

Young, Nicolás E., Alia J. Lesnek, Josh K. Cuzzone, Jason P. Briner, Jessica A. Badgeley, Alexandra Balter-Kennedy, Brandon L. Graham, et al. 2021. "In Situ Cosmogenic ^{10}Be–^{14}C–^{26}Al Measurements from Recently Deglaciated Bedrock as a New Tool to Decipher Changes in Greenland Ice Sheet Size." Climate of the Past 17 (1): 419–50. https://doi.org/10.5194/cp-17-419-2021.

FIGURES

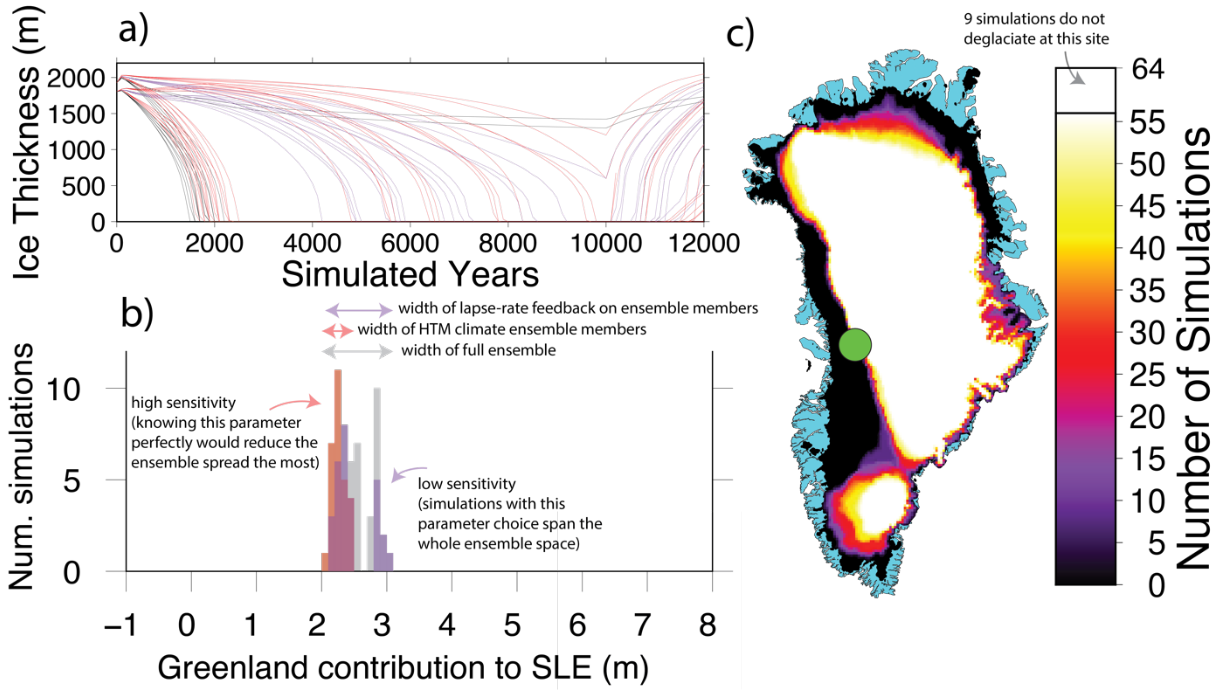

Figure 1. Ensemble design. An example of our results is shown for West Greenland. A) The thickness of ice for one location (the green dot in panel C) is plotted for all ensemble members. Each simulation is represented by one thin line. Simulations that reach thickness=0 at some point during the deglaciation are used to calculate sea-level potential for this site. Purple and red lines correspond to purple and red histograms in panel B. B) Histogram of outcomes for the location shown with the green dot in panel C. The contribution of Greenland to global sea level when this site becomes ice-free ranges from 2.0 meters to 3.2 meters. The ensemble members which all have the precipitation lapse rate turned off are superimposed on the histogram in purple. The ensemble members with a HTM climatology are superimposed in red. This site is most sensitive to HTM climate, because knowing that parameter with certainty would reduce the spread of the ensemble by the greatest amount. C) Greenland footprint associated with ice-free conditions for the location in West Greenland identified with a green dot. Black regions indicate that every simulation is ice-free at the same time that this location deglaciates, whereas white regions are still ice-covered in every simulation when this location becomes ice-free.

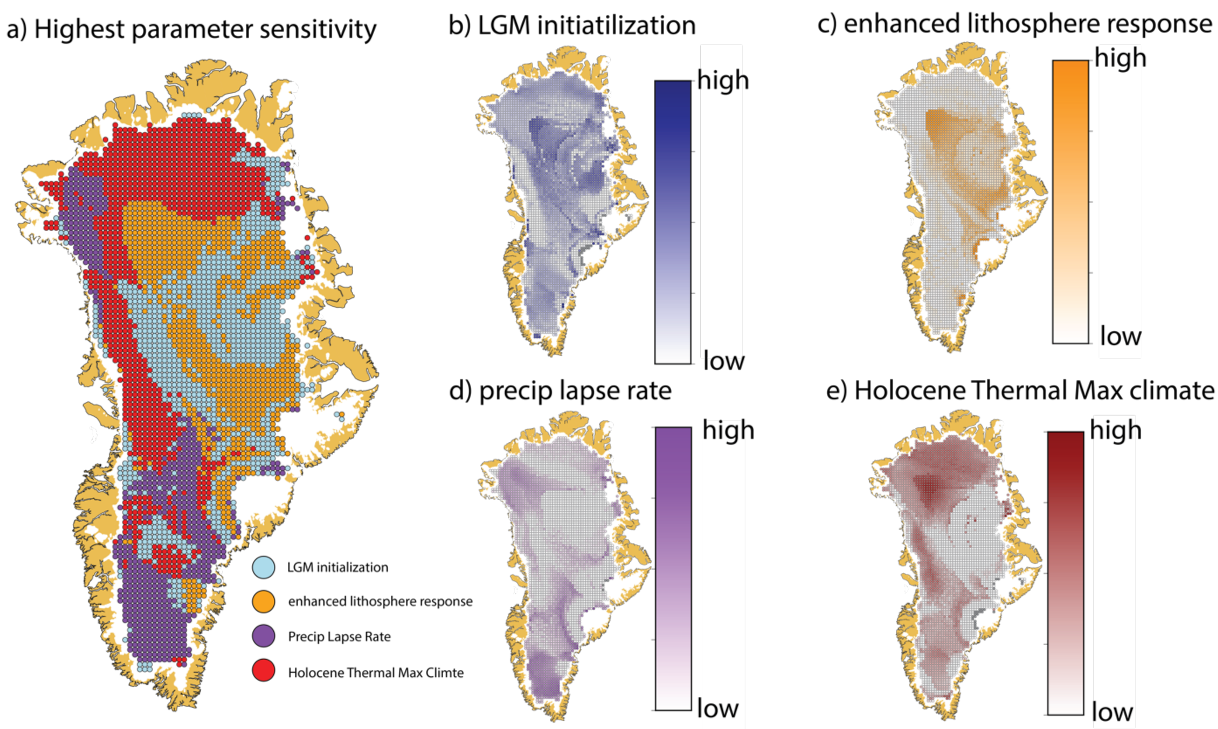

Figure 2. Parameter sensitivity test. A) Shows which ensemble parameter exerts the strongest control on the distribution of ice volume estimates when that location first becomes ice free. B) Sensitivity to starting the simulation from Last Glacial Maximum conditions. C) Sensitivity to a reduced response time of the elastic lithosphere relaxing asthenosphere solid-Earth model. D) Sensitivity to neglecting a precipitation lapse rate correction. E) Sensitivity to starting from a climatology from the Holocene Thermal Maximum.

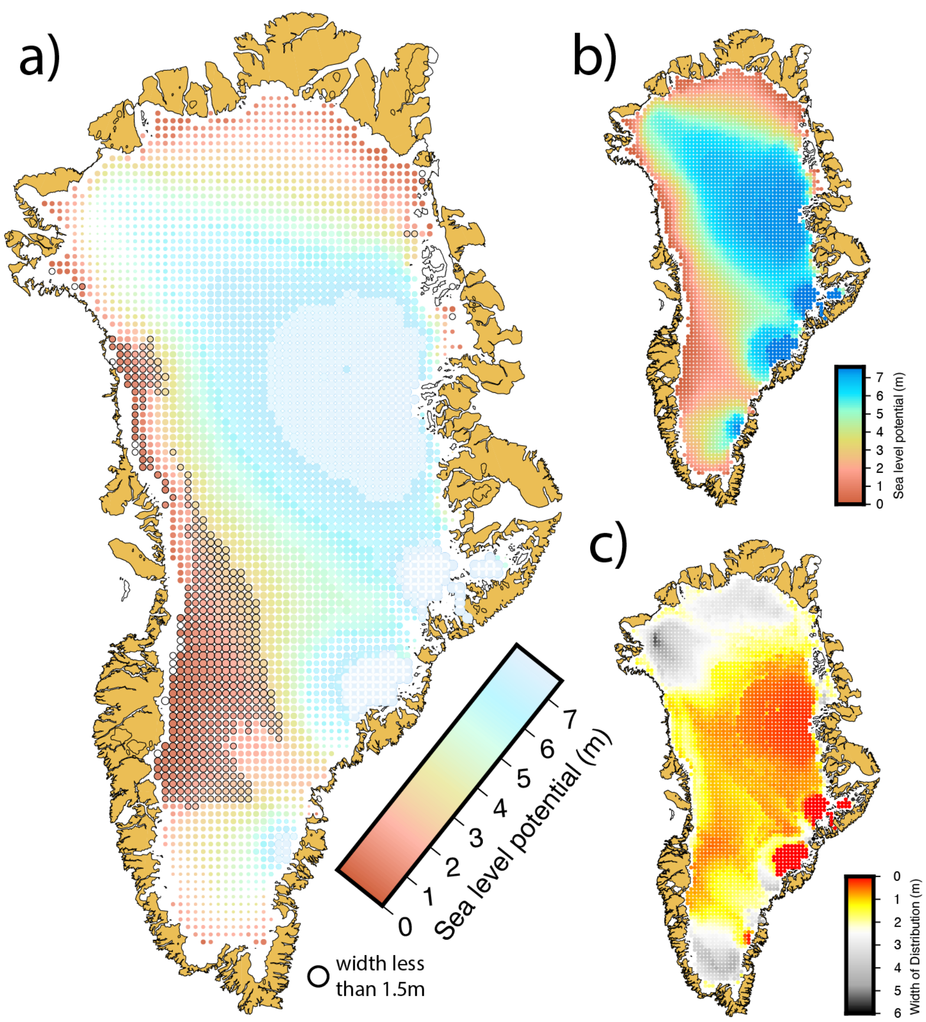

Figure 3. Greenland's sea level potential. a) Colors indicate sea level potential, defined as the mean amount that Greenland has contributed to global sea level when that grid cell has become ice-free. Size of each dot indicates the uncertainty (width of the full histogram as in Figure 1b). Black outline highlights regions where ice-free conditions are associated with median sea-level potential less? than 2 meters, and when the spread of the ensemble is less than 1.5 meters. b) Sea level potential only (meters sea level equivalent). c) Confidence: Histogram width only (meters sea level equivalent).

FIGURES FOR SUPPLEMENT

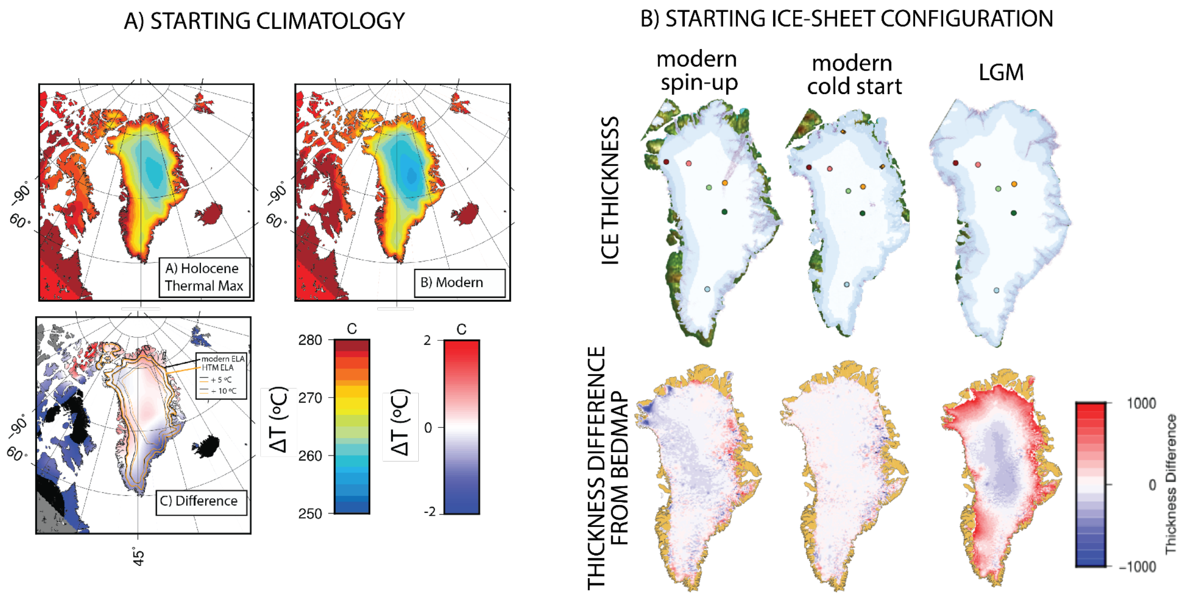

Supplemental Figure 1. Ice sheet model forcing and initialization. A) Two climatologies are used to initialize the climate forcing. The first is from the Holocene Thermal Maximum, and the second is modern (preindustrial). The difference between the two climatologies shows that the HTM climate is warmer in North and West Greenland by up to 2ºC. B) Three starting ice-sheet configurations are used in the ensemble: a modern ice-sheet spun up by running the model through a glacial cycle, a “cold start” from modern, and a Last Glacial Maximum ice sheet.

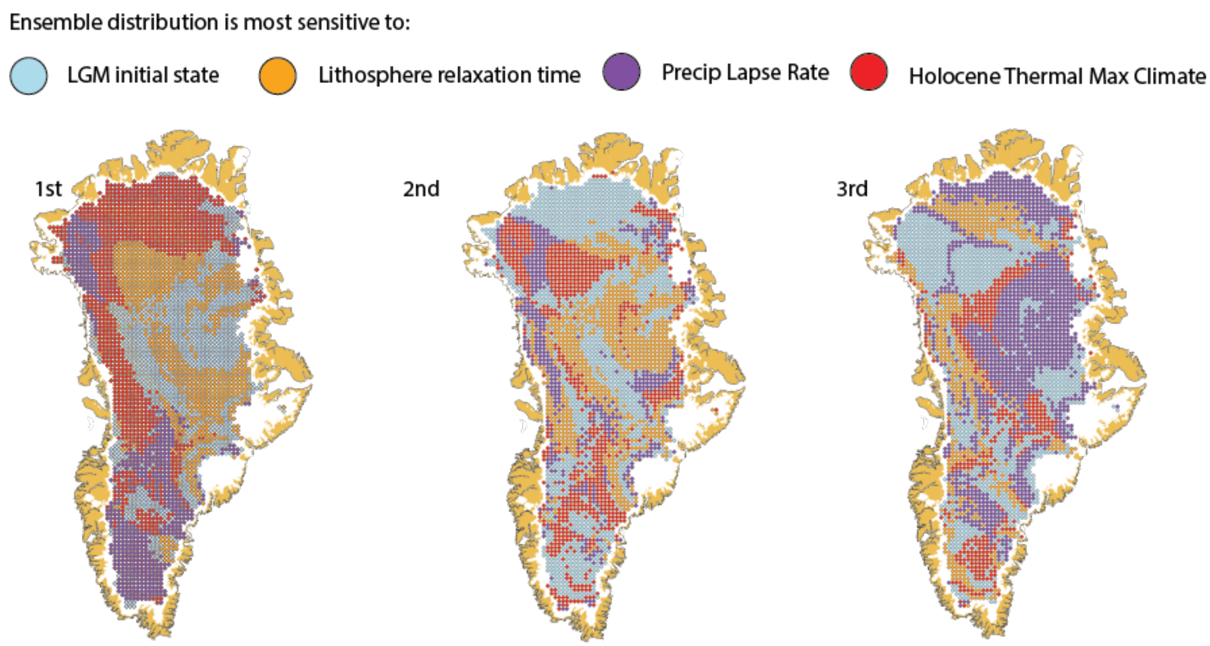

Supplemental Figure 2. Primary, secondary and tertiary parameter ranks. “1st” is the same as Figure 2a. To the right, the secondary and tertiary parameter sensitivities are shown. These describe, respectively, the second- and third-most important parameters for controlling the ensemble spread at any site.